

Supporting Information for:

Disruption of the *Plasmodium falciparum* life cycle through transcriptional reprogramming by inhibitors of Jumonji demethylases

Krista A. Matthews¹, Kossi M. Senagbe², Christopher A. Gonzales², Christopher Nötzel^{3,4}, Filipa Rijo-Ferreira⁵, Xinran Tong³, Natarajan V. Bhanu⁶, Celia Miguel-Blanco⁷, Maria Jose Lafuente-Monasterio⁷, Benjamin A. Garcia⁶, Björn F.C. Kafsack^{3,4} and Elisabeth D. Martinez^{1,2,8,*}

¹ Department of Pharmacology, The University of Texas Southwestern Medical Center, 6000 Harry Hines Blvd., Dallas, Texas, 75390 USA

² Hamon Center for Therapeutic Oncology Research, The University of Texas Southwestern Medical Center, 6000 Harry Hines Blvd., Dallas, Texas, 75390 USA

³ Department of Microbiology & Immunology, Weill Cornell Medicine, 1300 York Avenue, W-705, New York, New York, 10065 USA

⁴ Biochemistry, Cell & Molecular Biology Graduate Program, Weill Cornell Medicine, 1300 York Avenue, W-705, New York, New York, 10065 USA

⁵ Department of Neuroscience, The University of Texas Southwestern Medical Center, 6000 Harry Hines Blvd., Dallas, Texas, 75390 USA

⁶ Epigenetics Program, Department of Biochemistry and Biophysics, Perelman School of Medicine, University of Pennsylvania, 3400 Civic Center Blvd., Bldg. 421, Philadelphia, Pennsylvania, 19104 USA

⁷ GlaxoSmithKline, Tres Cantos Medicines Development Campus, Tres Cantos, P.T.M Severo Ochoa, Madrid, 28760 Spain

⁸ Lead contact

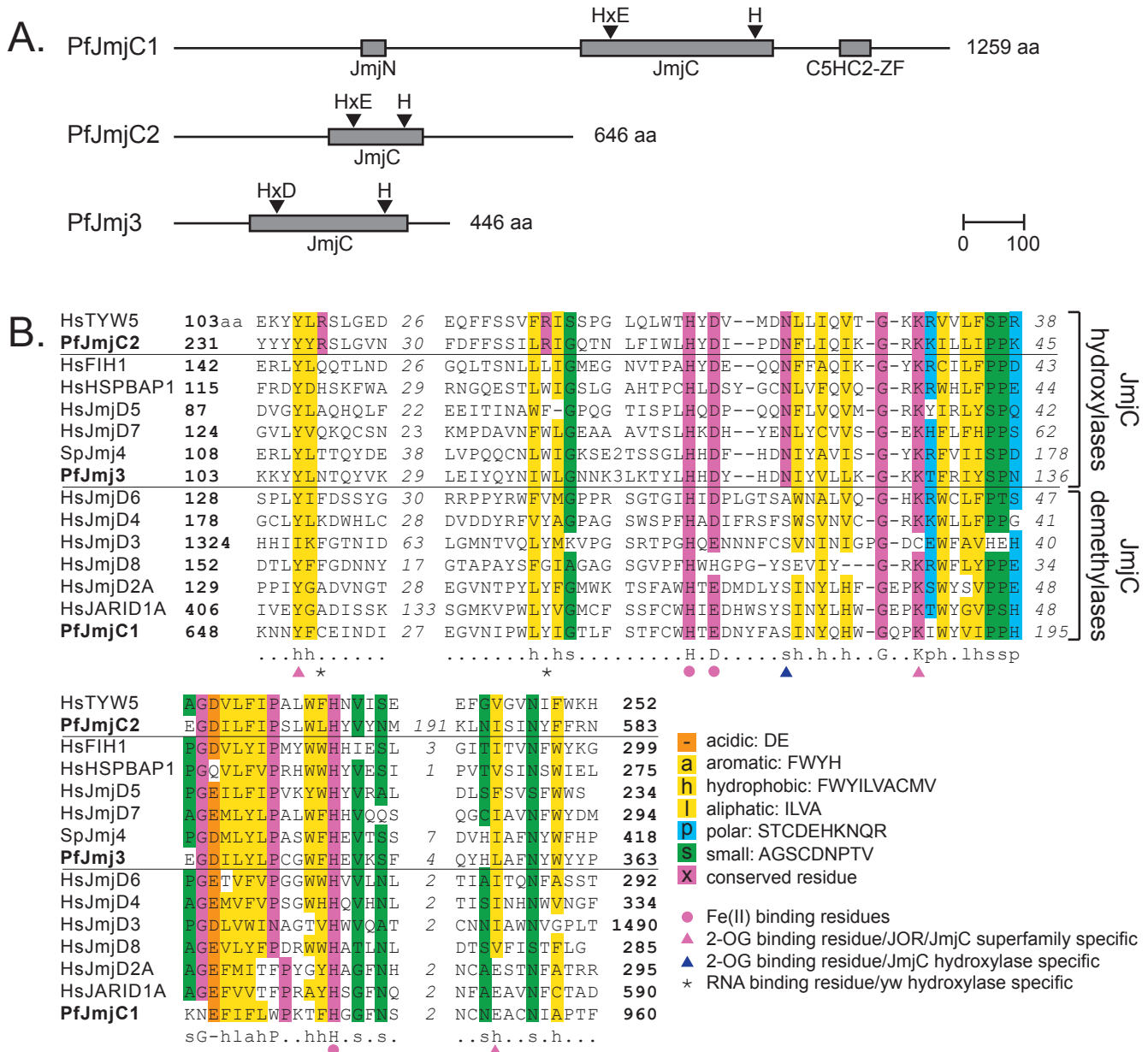
*correspondence to: elisabeth.martinez@utsouthwestern.edu

Pages S1 – S25

Figures S1 – S6

Tables S1 – S4

Figure S1



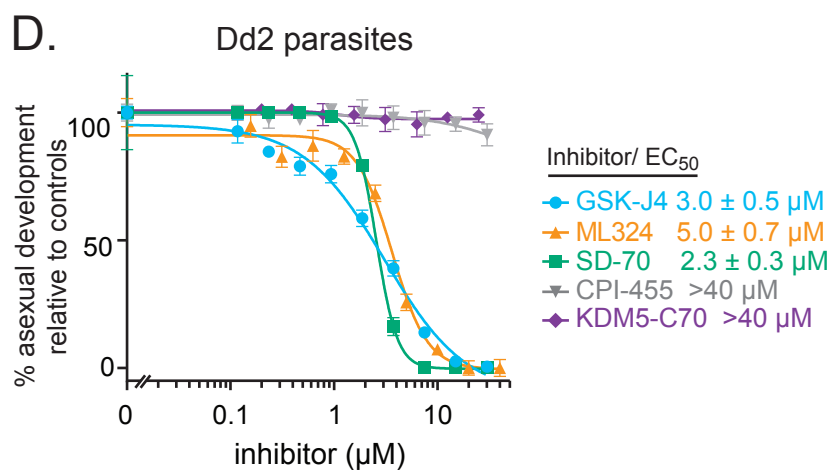
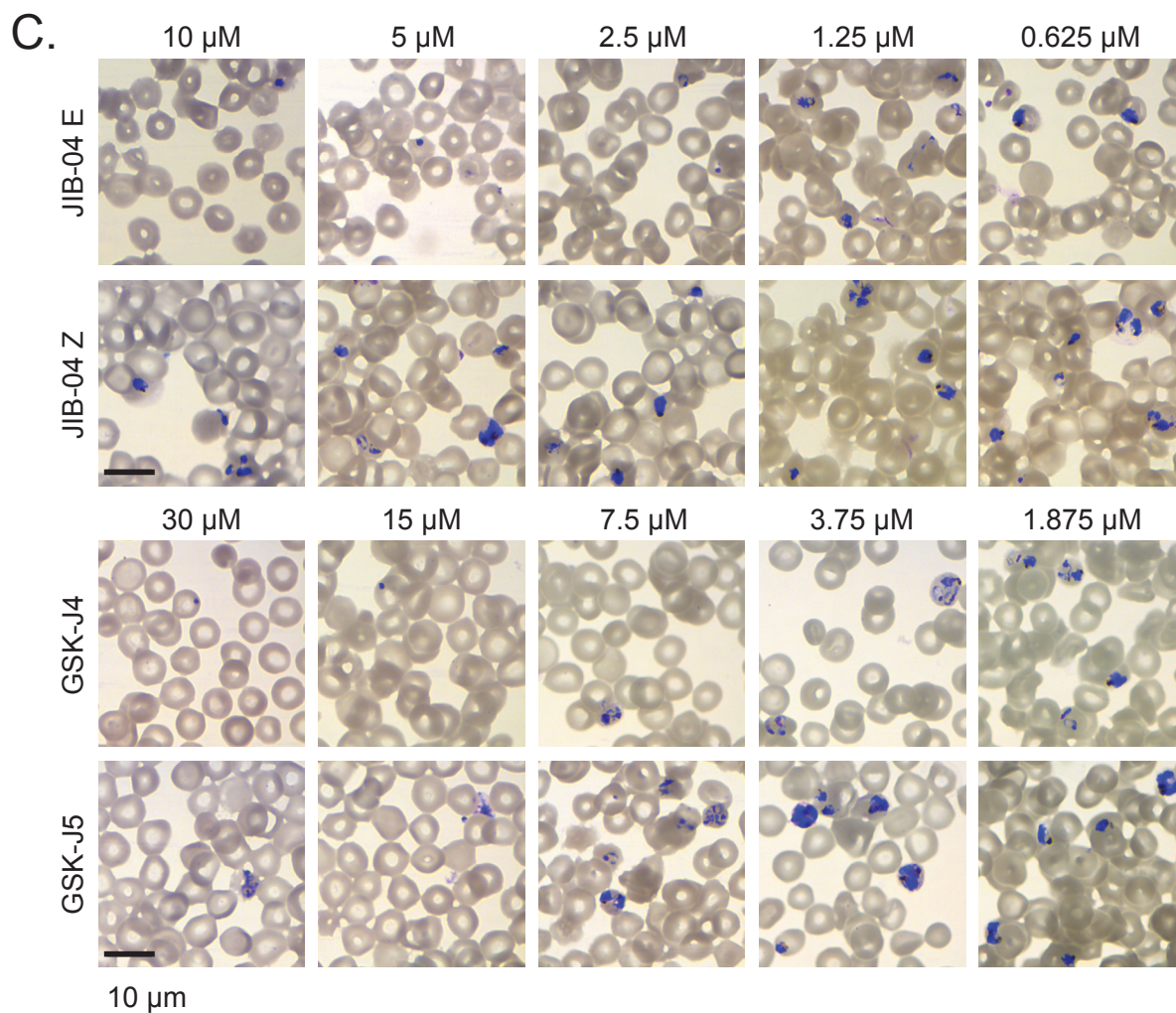
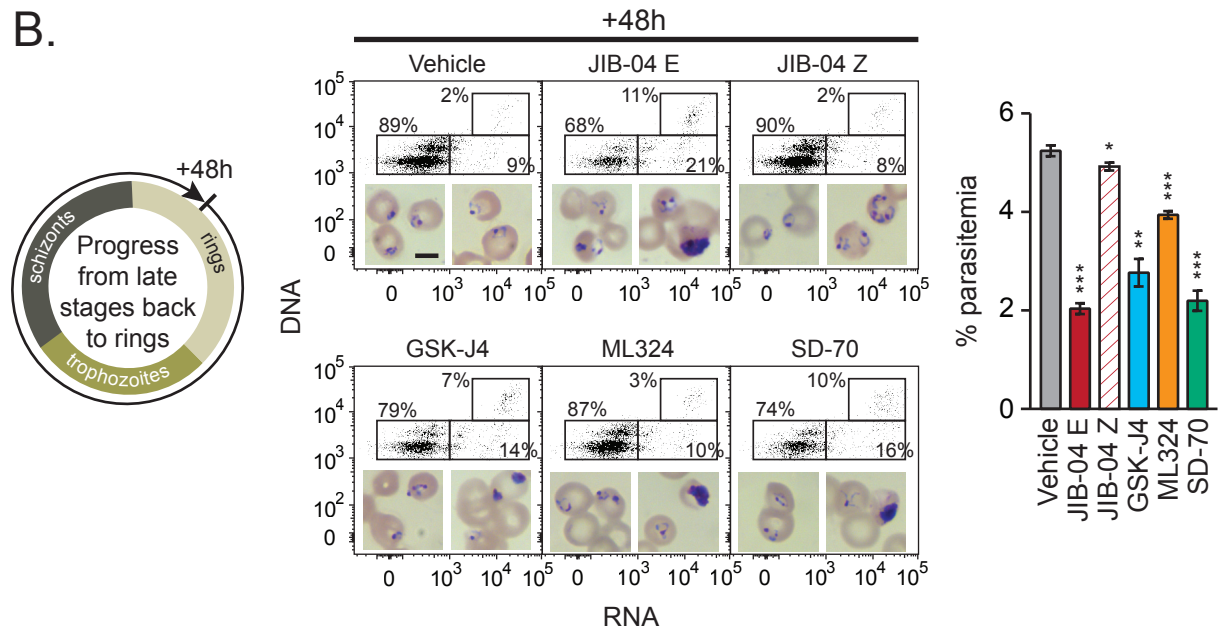
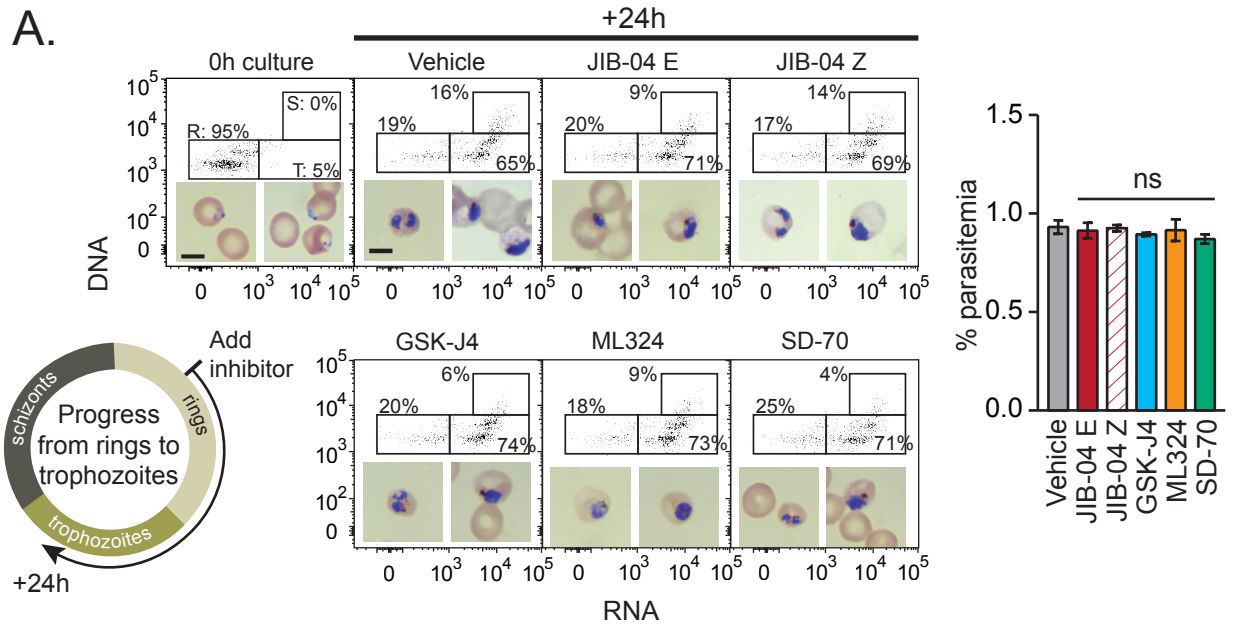


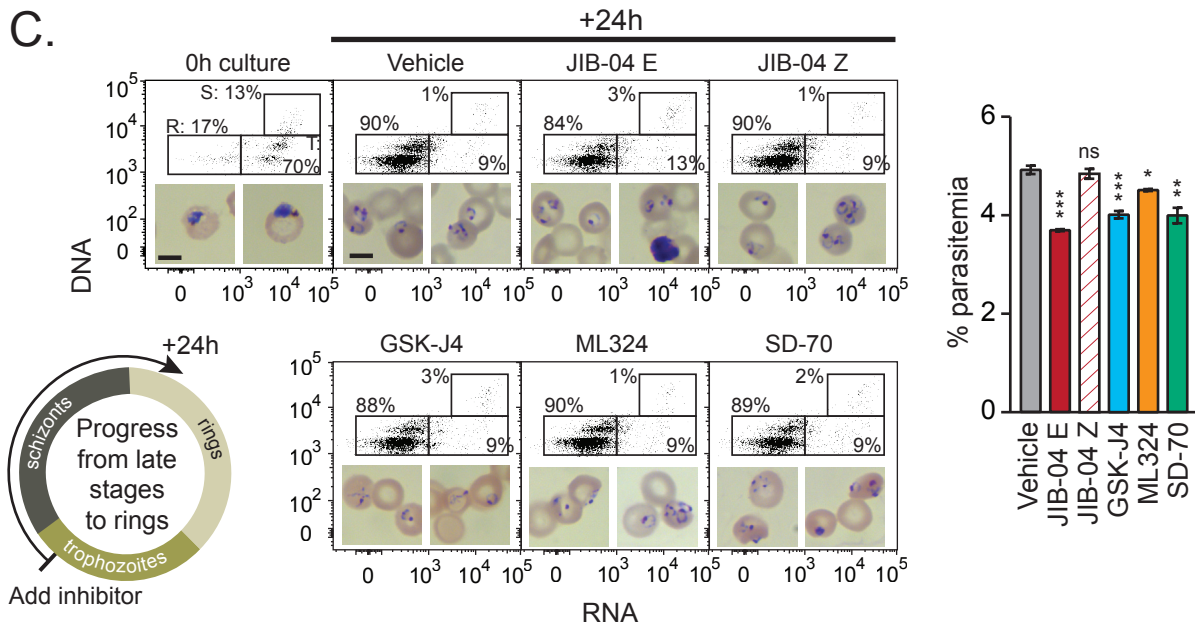
Figure S1. *Plasmodium falciparum* encodes three Jumonji C domain-containing domain proteins with conserved active site residues

A) Location of conserved domains and the Fe(II) coordinating residues (HxD/E, H) within the JmjC domain of *P. falciparum* proteins. Protein architectures were identified using the NCBI Conserved database. (JmjC, Jumonji C domain; JmjN, Jumonji N domain; C5HC2-ZF, C5HC2-zinc finger domain). **B)** Sequence alignment of JmjC domains from *Homo sapiens* (*Hs*) and *Saccharomyces pombe* (*Sp*) demonstrates that PfJmj proteins contain conserved residues including the Fe(II)-binding site (circles) and 2-OG-binding sites (triangles) required for enzymatic activity. RNA-binding residues (asterisks) in the Jumonji RNA hydroxylase, HsTYW5, are present in PfJmjC2, but not PfJmjC1 or PfJmj3. PfJmjC1 aligns with Jumonji histone demethylases, whereas PfJmjC2 and PfJmj3 align with JmjC hydroxylases. Alignment adapted from Iyer et al. 2010 (71). **C)** Representative images of Giemsa-stained 3D7 parasites treated with increasing concentrations of JIB-04 or GSK isomers after a 3 day exposure. Related to Figure 1. Scale bar = 10 μ m. **D)** Representative Jumonji inhibitor concentration curves against Dd2 asexual parasites. Synchronized rings were treated with GSK-J4 (cyan circles), ML324 (orange triangles), SD-70 (green squares), CPI-455 (grey inverted triangles), and KDM5-C70 (purple diamonds). Asexual development was measured using the standard 3 day growth assay as described in Methods and Materials and is presented as a percent of vehicle-treated controls. Inhibition curves are fitted to the mean of triplicate wells using nonlinear regression analysis. Error bars represent the standard deviation of technical triplicates. EC₅₀ concentrations (μ M) are presented as mean \pm SEM of the fitted inhibition curves from two or more independent experiments.

Figure S2



C.



D.

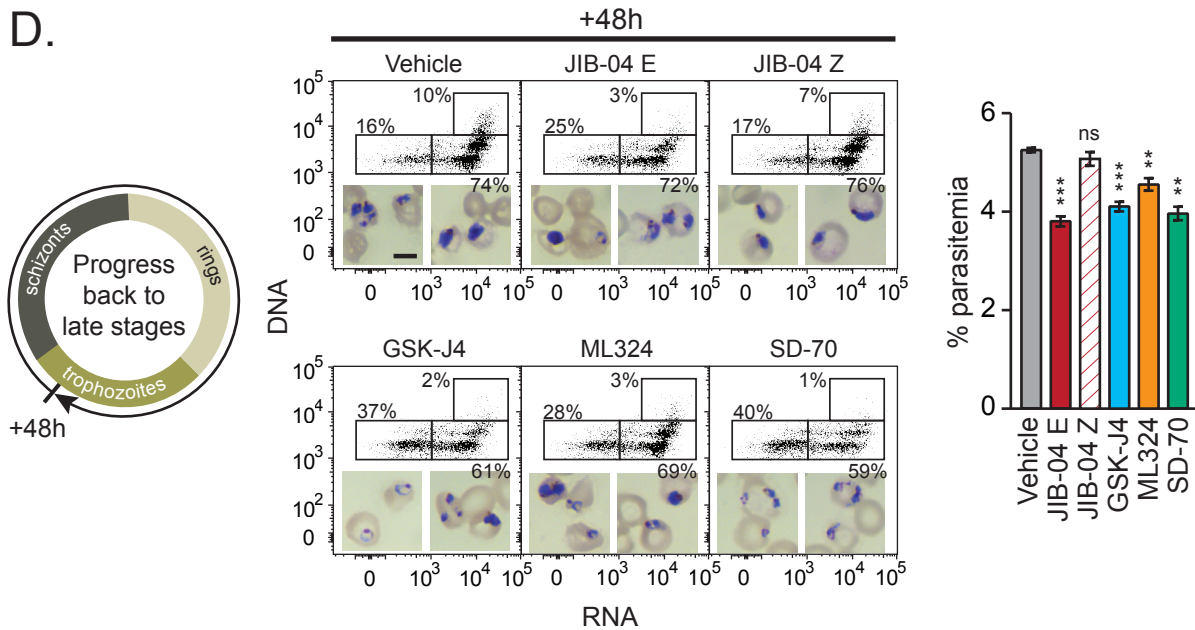
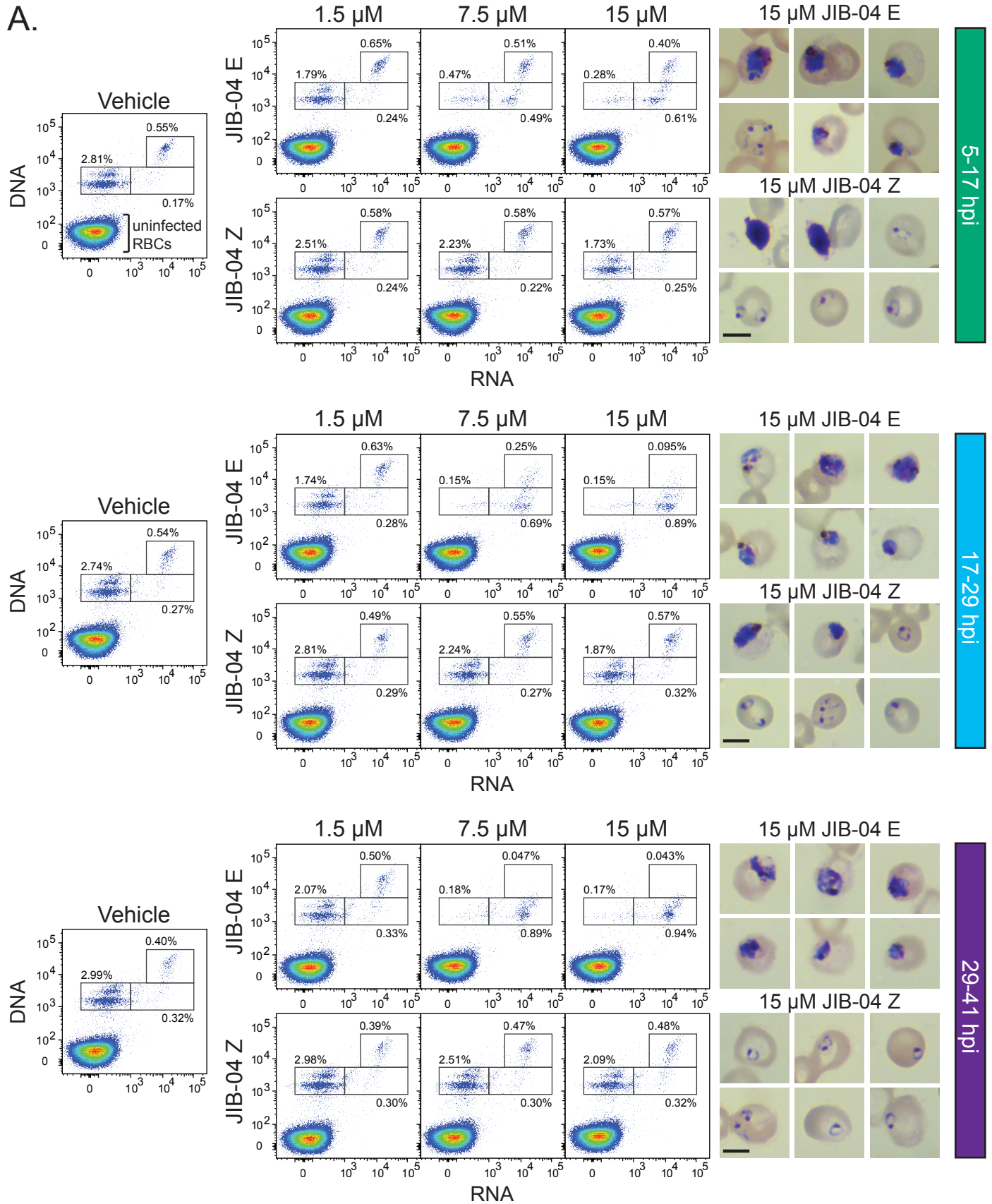


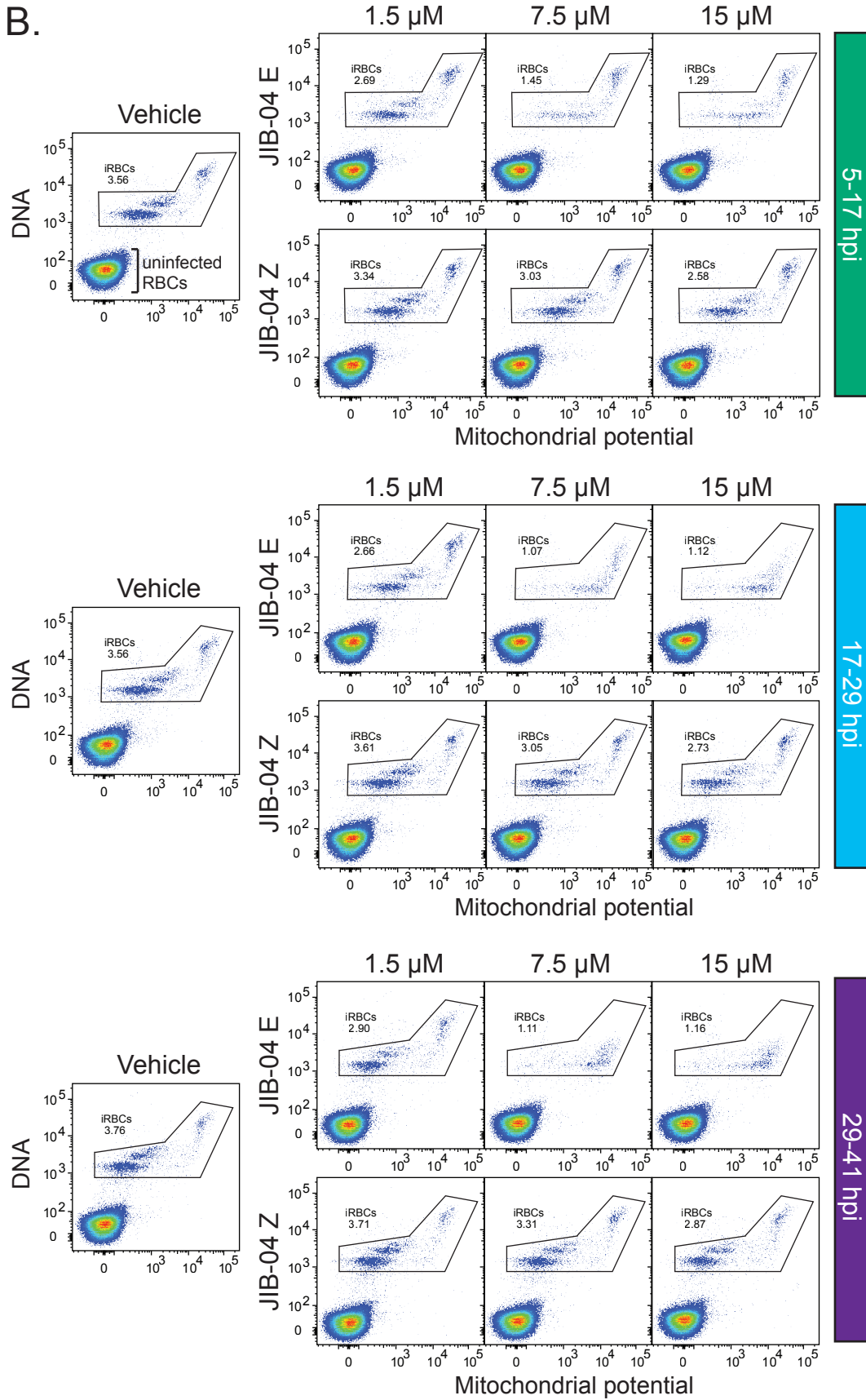
Figure S2. Jumonji inhibitors impair development of ring and late stage-treated parasites. Related to Figure 2.

Parasitemia and representative dot plots of ring (**A, B**) and trophozoite (**C, D**) stage parasites after 24 h (**A, C**) and 48 h (**B, D**) exposure to vehicle or Jumonji inhibitors corresponding to Figure 2. First, infected RBCs with live parasites were defined as Hoechst/DNA-positive and DiIC₁(5)/mitochondrial potential-positive according to Grimberg (78) (data not shown). Then, parasite stages were separated using Hoechst/DNA and thiazole orange/RNA signals: ring stage parasites were defined as DNA-positive/RNA-negative; trophozoites and early schizonts were defined as <3N DNA-positive/RNA-positive; schizonts were defined at >3N DNA-positive /RNA-positive. Percentages represent the average distribution of parasites within each gate as a total of infected RBCs across three technical replicates. Bar graphs represent the mean \pm SD of three wells from 1 of 2 independent experiments. *p* values are calculated using a *t* test between vehicle- and inhibitor-treated samples. ns: nonsignificant, * *p*<0.05, ** *p*<0.01, *** *p*<0.001. Scale bar = 5 μ m.

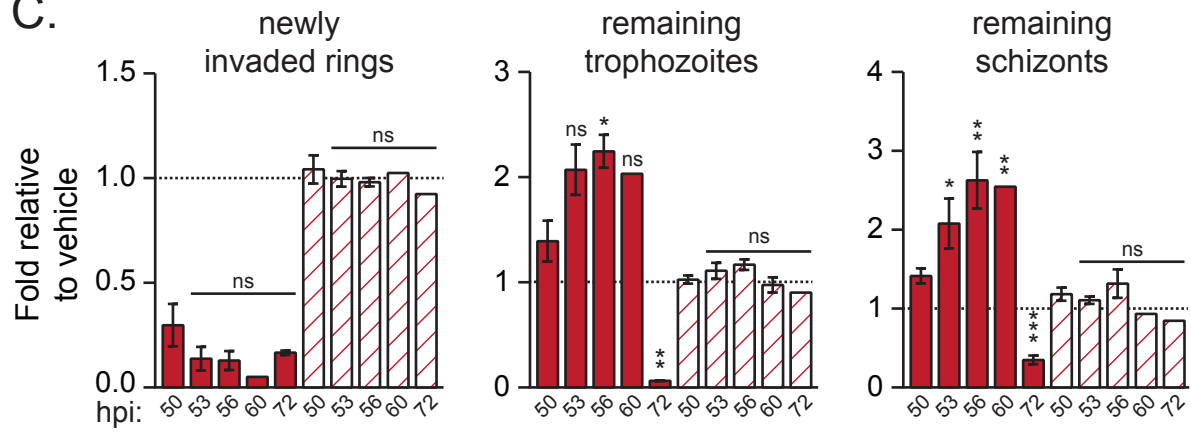
Figure S3



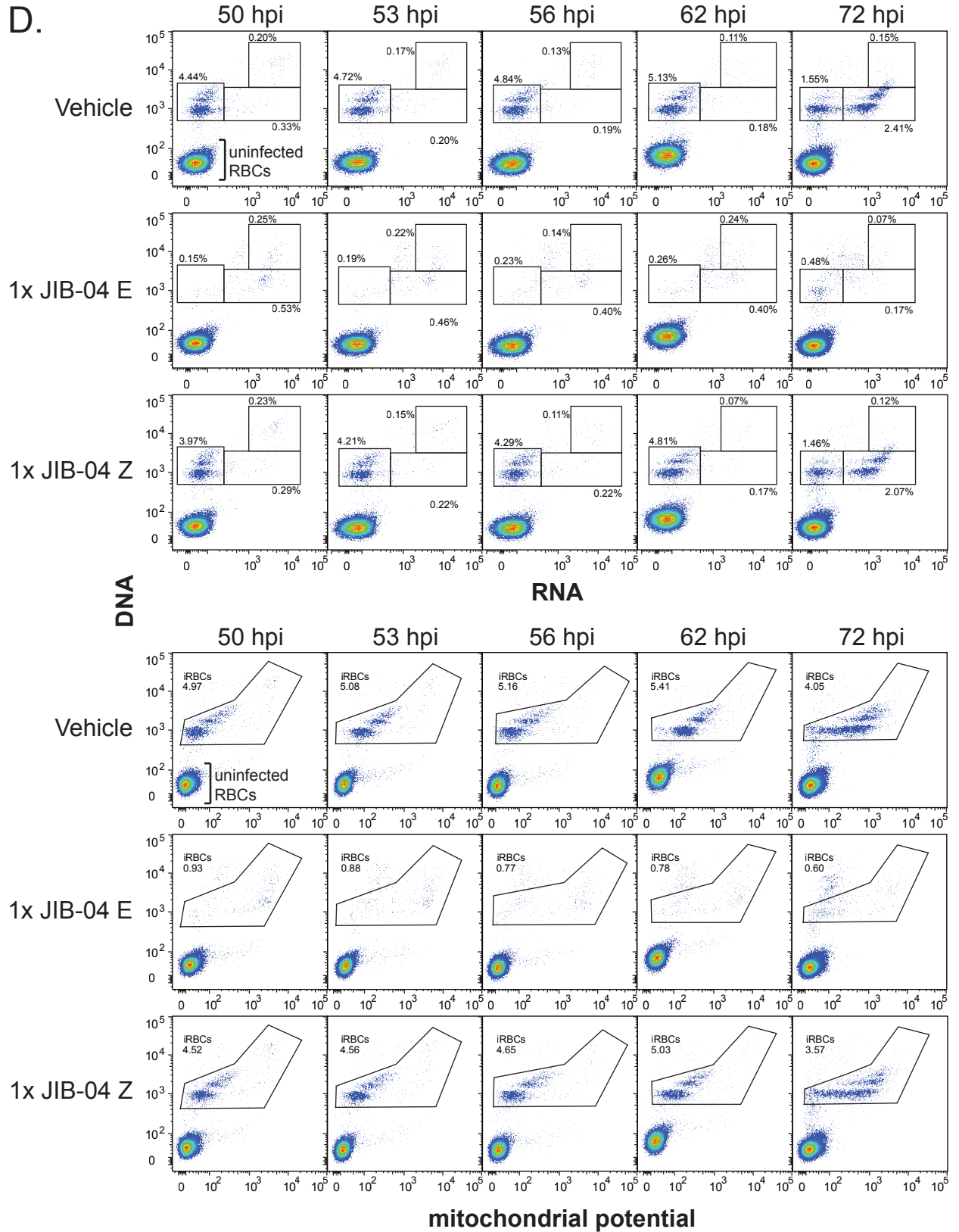
B.



C.



D.



E.

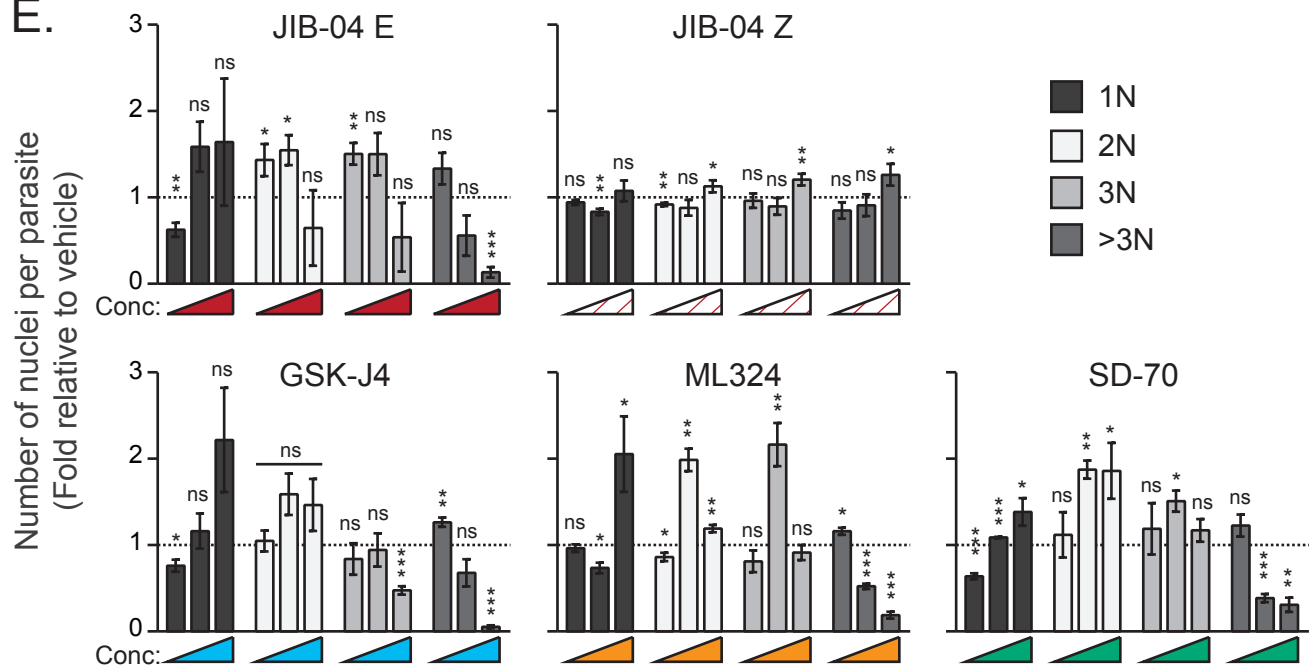


Figure S3. Short term exposure to JIB-04 E impairs IDC. Representative dot plots of data in Figure 3.

Representative dot plots of treated-parasites at 50 hpi stained with either Hoechst 33342 (DNA) and **A)** thiazole orange (RNA) or **B)** DiIC₁(5) (mitochondrial membrane potential). Uninfected RBCs cluster in the lower left quadrant. Percentages represent the **A)** distribution of parasites within each gate as a total of RBCs or **B)** total parasitemia. Representative images of Giemsa-stained parasites at 50 hpi from wells treated with 10x EC₅₀ JIB-04 E or Z. Scale bar: 5 μ m. **C & D)** Synchronized parasites as in Figure 3 were exposed to vehicle, 1x JIB-04 E, or 1x JIB-04 Z during the 29-41 hpi treatment period. Parasite progression and completion of the IDC (reinvasion) were monitored by flow cytometry as described in Figure 3 at 50, 53, 56, 60, and 72 hpi. **C)** Data are presented as fold change relative to vehicle-treated controls and represent the mean \pm SEM of 2 independent experiments (except 60 hpi for JIB-04 E and Z and 72 hpi for JIB-04 Z which are from one experiment). *p* values are calculated using a *t* test between vehicle- and inhibitor-treated samples. ns: nonsignificant, * *p*<0.05, ** *p*<0.01, *** *p*<0.001. **D)** Representative dot plots of treated-parasites stained at defined time points with either Hoechst 33342 (DNA) and thiazole orange (RNA) or DiIC₁(5) (mitochondrial membrane potential). Uninfected RBCs cluster in the lower left quadrant. Percentages represent the distribution of parasites within each gate as a total of RBCs (for DNA vs RNA) or total parasitemia (for DNA vs mitochondrial potential). Late stage parasites (>3N) with positive DNA staining, but no mitochondrial signal are considered dead. We cannot determine viability of early stage parasites based on this method. **E)** Analysis of the DNA content from the remaining late stage parasites (remaining trophozoite and schizont gates from 29-41 hpi treated parasites) at 50 hpi suggests that Jumonji inhibitors cause a cell cycle arrest phenotype. Increasing concentrations of Jumonji inhibitors (1x, 5x, and 10x EC₅₀ concentrations) result in a greater number of remaining late stage parasites with 1N, 2N, or 3N nuclei and a corresponding decrease in segmented schizonts (>3N nuclei). Data are presented as fold change relative to vehicle-treated controls and represent the mean \pm SEM of 3-4 independent experiments. *p* values are calculated using a *t* test between vehicle- and inhibitor-treated samples. ns: nonsignificant, * *p*<0.05, ** *p*<0.01, *** *p*<0.001.

Figure S4

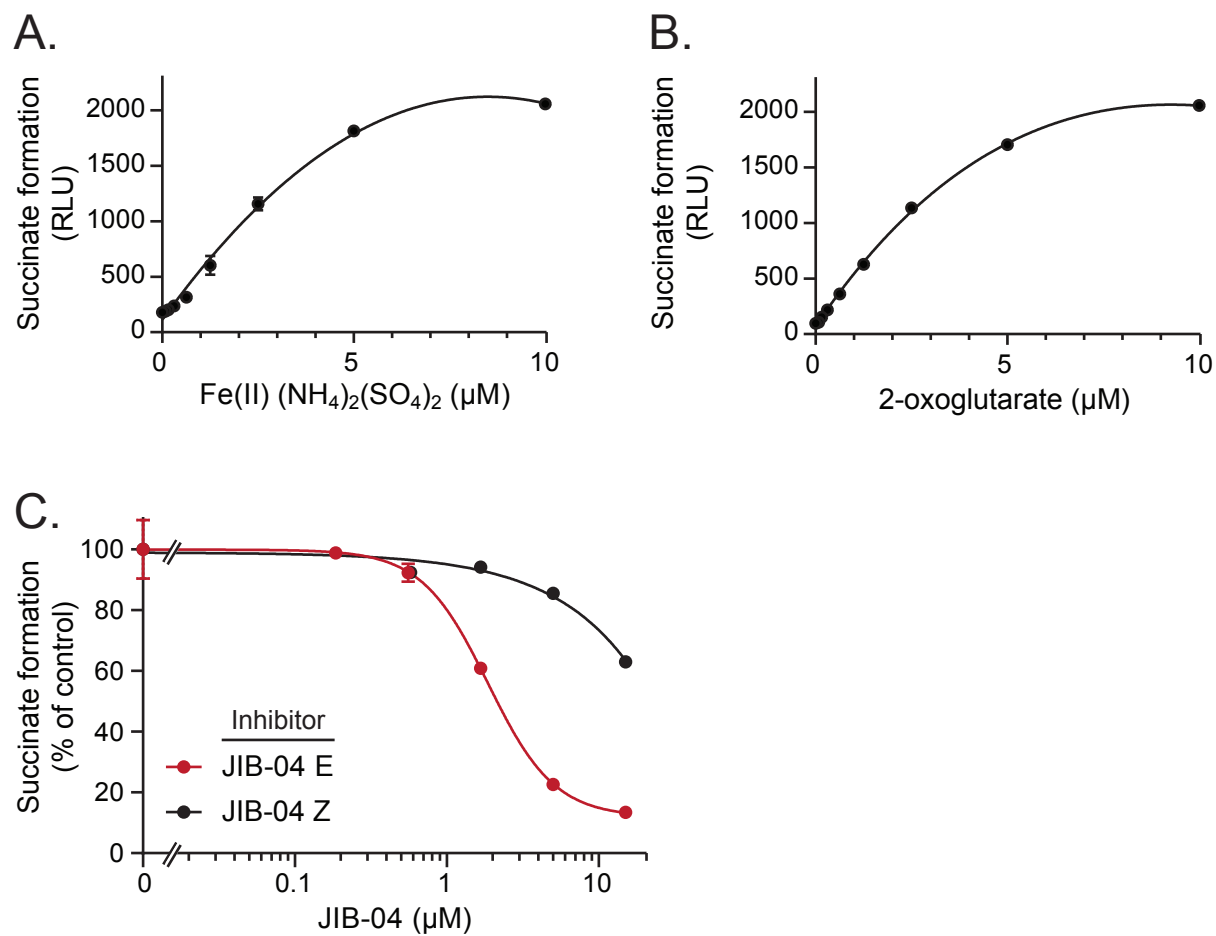
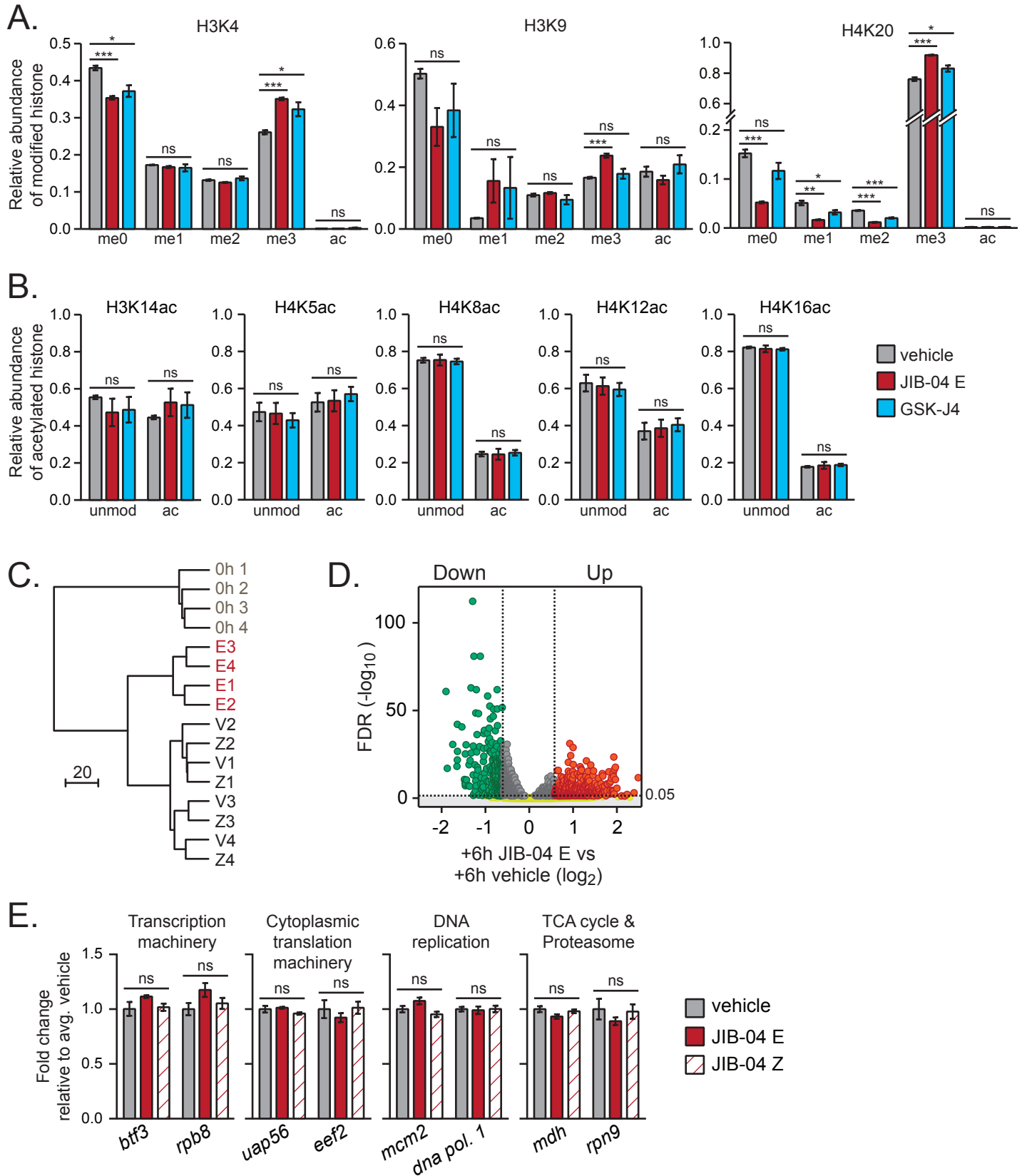


Figure S4. Recombinant PfJmj3 enzymatic activity is dependent on Fe(II) and 2-OG concentration. Related to Figure 4.

Concentration curves of **A)** Fe(II) and **B)** 2-oxoglutarate. Succinate-Glo JmjC Demethylase/Hydroxylase assays were performed with 0.4 μ g recombinant MBP-HIS₆-PfJmj3 incubated with 50 mM HEPES, pH 7.5, 100 μ M ascorbate, and two-fold serial dilutions of **A)** Fe(II) or **B)** 2-OG (10 μ M max) for 1 hour at room temperature. Data are the mean \pm SD of 2 technical replicates from 1 of 2 independent experiments. Non-linear curves were fit using GraphPad Prism. RLU: relative luciferase units. **C)** Inhibition of succinate production in the presence of increasing concentrations of JIB-04 E or Z isomers. Succinate-Glo JmjC Demethylase/Hydroxylase assay performed with 0.4 μ g of recombinant MBP-HIS₆-PfJmj3 in 50 mM HEPES, pH 7.5, 5 μ M ascorbate, 0.5 μ M Fe(II), and 2.5 μ M 2-OG in the presence of 0 – 15 μ M inhibitor for 1 hour at room temperature. Data is plotted as a percentage of the activity with 0 μ M inhibitor (100%) and represent the mean \pm SD of 2 technical replicates from 1 of 2 independent experiments. A non-linear curve ([Inhibitor] vs. response - Variable slope (four parameters)) was fit using GraphPad Prism.

Figure S5



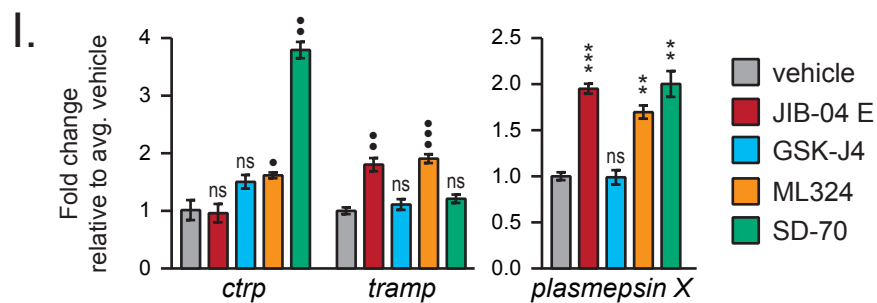
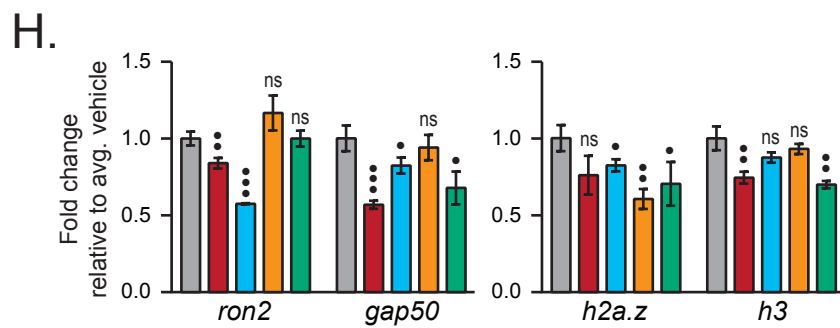
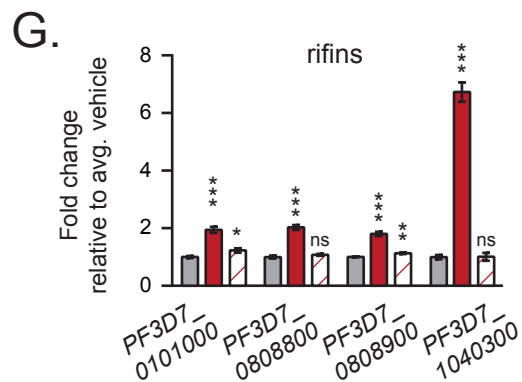
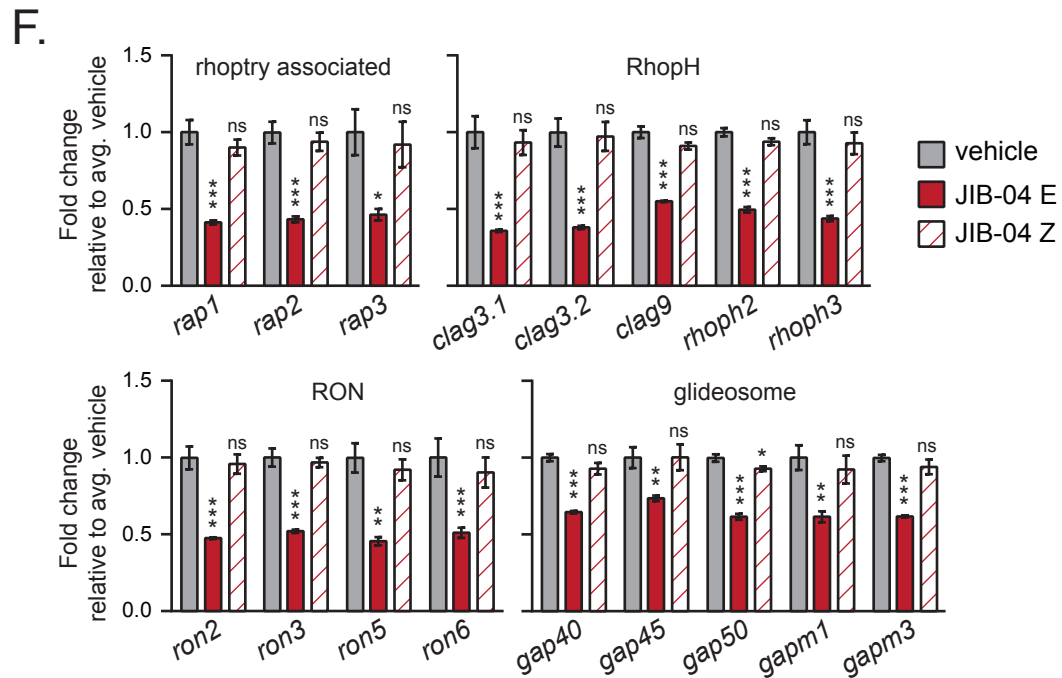


Figure S5. Jumonji inhibitors deregulate transcription of a subset of genes and do not alter global histone acetylation during IDC. Related to Figure 5.

A) Relative abundance of histone methylation and acetylation on H3K4, H3K9, and H4K20 in 29 hpi parasites treated with vehicle, 4.5 μ M JIB-04 E, or 9 μ M of GSK-J4 for 6 h. Bar graphs represent the mean \pm SEM of three biological replicates. **B)** Relative abundance of histone acetylation on H3 and H4 lysine residues in 29 hpi parasites treated with vehicle, JIB-04 E, or GSK-J4 as above. Bar graphs represent the mean \pm SEM of three replicates. *p* values are calculated using a *t* test between vehicle- and inhibitor-treated samples. **C)** Hierarchical clustering of RNA sequencing results from 29 hpi parasites (0h) treated with vehicle (V), 4.5 μ M JIB-04 E (E) or 4.5 μ M inactive Z isomer (Z) for 6 h (four replicate/treatment). **D)** Volcano plot of the significance ($-\log_{10}(\text{FDR})$) versus fold change (\log_2) for comparison of JIB-04 E- versus vehicle-treated parasites at 6 h. Green and red dots represent genes whose expression significantly decreased or increased greater than 1.5-fold between JIB-04 E- and vehicle-treated parasites, respectively. Genes that did not differ between the treatments are colored grey and genes that did not meet the 0.05 FDR cutoff are yellow. **E-G)** Examples of genes whose expression showed **E)** no difference, **F)** downregulation, or **G)** upregulation when treated with JIB-04 E compared to controls. Data are the mean \pm SEM of four replicates. *p* values are calculated using a *t* test between vehicle- and inhibitor-treated samples. **H-I)** qRT-PCR analysis of select genes **H)** downregulated or **I)** upregulated from 29 hpi parasites treated with vehicle or 3x EC₅₀ concentrations of Jumonji inhibitors for 6 h. Bar graph for *plasmepsin X* represents the mean \pm SEM of the fold change relative to vehicle from three biological replicates, whereas *ron2*, *gap50*, *h2a.z*, *h3*, *ctrp*, and *tramp* are the mean \pm SD of technical replicates from one sample set. *p* values are calculated using a *t* test between vehicle- and inhibitor-treated samples (* represents *p* values of fold changes across three experiments and • across technical replicates within one experiment). * *p*<0.05, ** *p*<0.01, *** *p*<0.001.

Figure S6

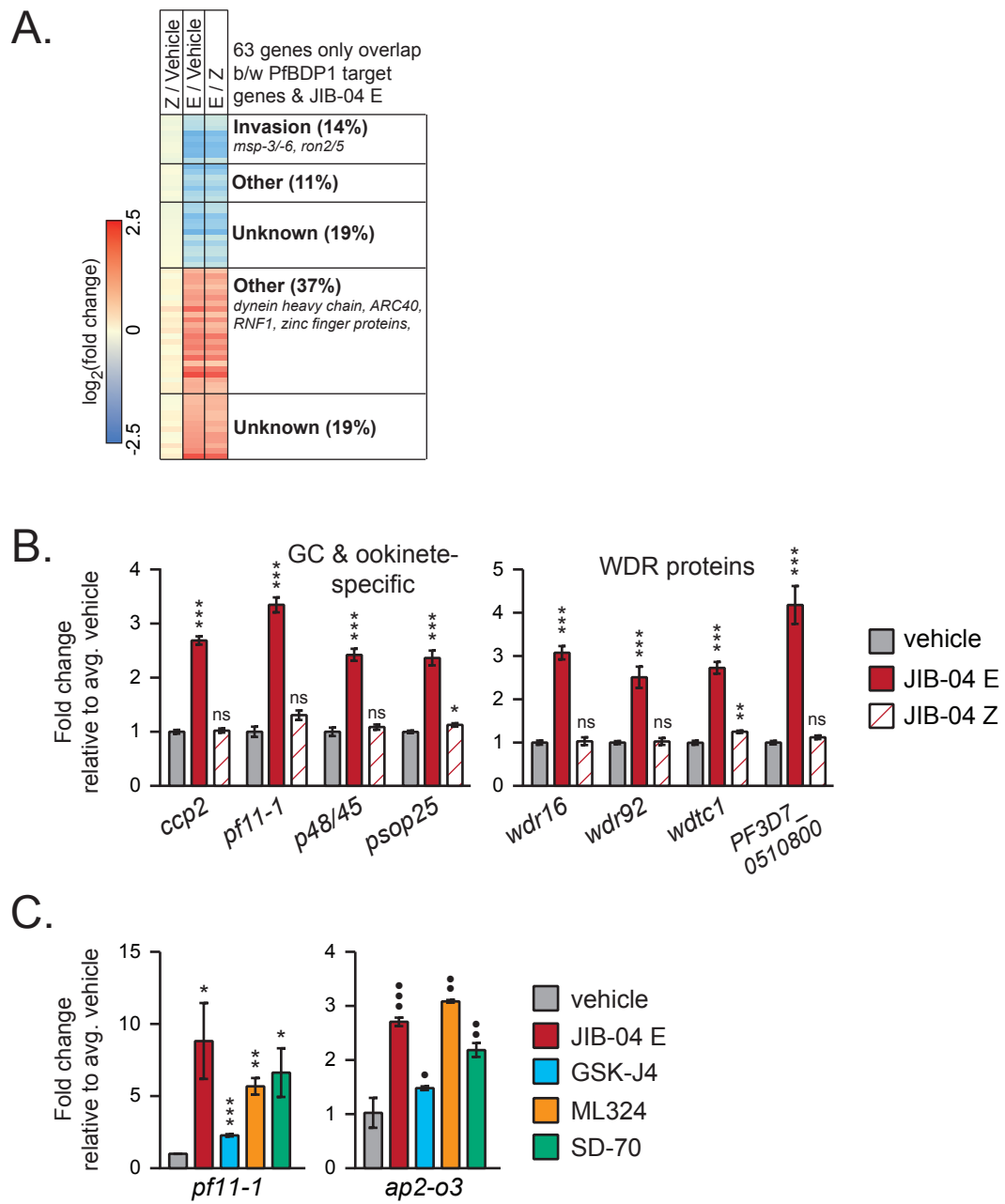


Figure S6. Downregulation of PfBDP1 target gene expression and upregulation of gametocyte and ookinete specific genes by Jumonji inhibitors. Related to Figure 6.

Heat map of differential expression between JIB-04 E and controls of an additional 63 PfBDP-1 target genes that overlap with genes downregulated by JIB-04 E, but are not targets of PfAP2-I. **B)** Examples of gametocyte- and ookinete-specific genes whose expression was upregulated when treated with JIB-04 E compared to controls. Data are the mean \pm SEM of four replicates. *p* values are calculated using a *t* test between vehicle- and inhibitor-treated samples. **C)** qRT-PCR analysis of select gametocyte- and ookinete-specific genes from 29 hpi parasites treated with vehicle or 3x EC₅₀ concentrations of Jumonji inhibitors for 6 h. Bar graph for *pfl1-1* represents the mean \pm SEM of the fold change relative to vehicle from three biological replicates, whereas *ap2-o3* is the mean \pm SD of technical replicates from one sample set. *p* values are calculated using a *t* test between vehicle- and inhibitor-treated samples (* represents *p* values of fold changes across three experiments and • across technical replicates within one experiment). ns: nonsignificant, * *p*<0.05, ** *p*<0.01, *** *p*<0.001.

Table S1

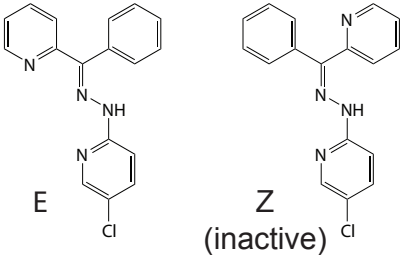
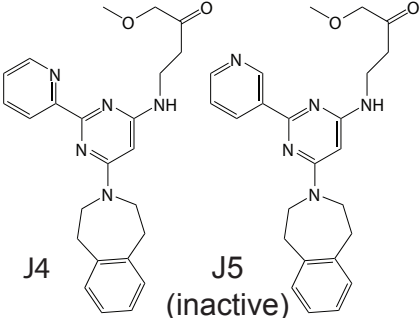
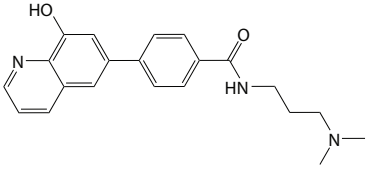
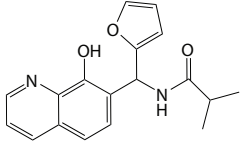
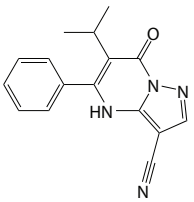
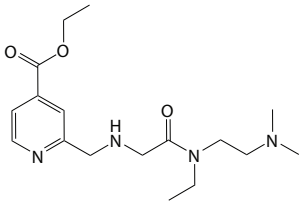
Inhibitor	Structure	Mammalian Jmj KDM tested	Reported IC ₅₀ (nM) / assay / histone substrate
JIB-04	 <p>E (active) Z (inactive)</p>	JARID1A JMJD2/KDM4C JMJD3/KDM6	230 nM (ELISA on H3K4me3) 350 - 1100 nM (ELISA on H3K9me3) 855 nM (ELISA on H3K27me3)
		Wang et al. 2013	
GSK-J4	 <p>J4 (active) J5 (inactive)</p>	JMJD3/KDM6	60 nM (AlphaScreen on H3K27me3)
		Kruidenier et al. 2012	
ML324		JMJD2/KDM4C	920 nM (AlphaScreen on H3K9me3)
		Rai et al. 2010	
SD-70		JMJD2/KDM4C	~30 nM (Immunoblot on H3K9me2) not determined for H3K9me3
		Jin et al. 2014	
CPI-455		JARID1	10 nM (TR-FRET on H3K4me3)
		Vinogradova et al. 2016	
KDM5-C70		JARID1	300 - 500 nM (AlphaScreen on H3K4me3)
		Horton et al. 2016 Johansson et al. 2016	

Table S1. Inhibitors of mammalian Jumonji histone demethylases used in this study

Structure of Jumonji inhibitors and inactive isomers used in this study. Reported IC₅₀ concentrations for mammalian Jmj enzymes tested with specified inhibitors along with the *in vitro* assay and histone peptide substrate used.

Table S2. Primers used for QRT-PCR.

Gene ID	Gene Name	Forward/Reverse Primer Sequence (5' → 3')
PF3D7_0302500	cytoadherence linked asexual protein 3.1 (Clag 3.1)	CTTCACTCACGGACTTGCTG TGCAGGACCAAATCCTCCAG
PF3D7_0315200	circumsporozoite- and TRAP-related protein (CTRP)	GGTGTAGCTGCTGCTGAAGA TGGCAATGTGTTGGTGTGGA
PF3D7_0320900	H2A.Z	AGCCATTAGAGGTGACGAAGA TTGAGCTGTTGGGGGAAGTG
PF3D7_0604100	AP2 domain transcription factor, SPE2-interacting protein (SIP2)	AGAATTGAAAGAGAATGGAGAGTAGAG TTTGTGCTTCATCATTACCTACTTTT
PF3D7_0610400	H3	TCAACTGCTGGTAAAGCCCC ACCAGCAGAGATTGGAGCTG
PF3D7_0615100	enoyl-ACP reductase (Enr/FabI)	GGATACGGGTGGGGTATTGC AGCGTCAAAGGGTAGCATGT
PF3D7_0626300	beta-ketoacyl-ACP synthase I/II (FabB/F)	TCATTATGCAGTCGCAGCCA AGTCCACCTATGCCACTACCT
PF3D7_0717700	serine tRNA ligase	ATGGAACAATGGTAGCTGCAC TGGGCGCAATTTTTCAGGAAC
PF3D7_0718000	dynein heavy chain	GATCACGAGGACAGGGAACA ACGGTCTCCGTTTTTCCTGT
PF3D7_0808200	plasmepsin X	ATGCCTGCCTACATGCAAATC AGGTCTACTTTCTGTGCCTCG
PF3D7_0815900	dihydrolipoyl dehydrogenase (aLipDH)	GGTTGTGGTGTGGAGGACA CGCTTTGCTTGGTATACAGCC
PF3D7_0905300	dynein heavy chain	CCTGTGCTCAAGCTTTGGGT ACGGTCTCCGTTTTTCCTGT
PF3D7_0918000	glideosome-associated protein 50 (GAP50)	CGTCTTTGGGTGATTGGGGT TCCATGCTGGATCATTTAAGCC
PF3D7_1038400	Pf11-1	AAGACAAAGGTGGCGGTGAA TCACCTCCTGCACTATCCCC
PF3D7_1218000	thrombospondin-related apical membrane protein (TRAMP)	AAATCATCTGGAGCTTTCCGT AGACCATTCTCCCCATTCTGA
PF3D7_1410400	rhoptry-associated protein 1 (RAP1)	TCAGCTAGTCCACATGGTGAATC CTTCTTCGTCGGCACCTACA
PF3D7_1429200	AP2-O3	CGGGTGTTTGGTATGATTTGC GGCTAACTTCCTTGCTTCATG
PF3D7_1452000	rhoptry neck protein 2 (RON2)	ATAGGTGCAGGACCAGTAGC AGCTAAACCTGCCATAGGAGC

Table S3. Transcriptome analysis and GO-terms of genes deregulated by JIB-04 E. Related to Figures 5 & 6.

Resulting genes from RNA sequencing showing >1.5-fold change in JIB-04 E cultures relative to vehicle and Z isomer (presented as log₂(FC) after 6 h treatment using a FDR cutoff of <0.05. Gene IDs are based on PlasmoDB version 34. Also included are average expression values (RPKM) for the starting 29 hpi parasite cultures (0h) and parasites cultures after 6 h treatment vehicle or JIB-04 isomers (+6h). GO analysis of differentially expressed genes based on molecular function, biological processes, and cellular component. This file includes four tabs: **1)** RNA-Seq Down, contains genes downregulated by JIB-04 and the analysis of how these genes overlap with PfBDP1 targets (by ChIP-seq and by knock down) (51) and PfAP2-I targets (50); **2)** GO terms-Down, contains annotation for the 235 genes downregulated by JIB-04 E; **3)** RNA-Seq Up, contains genes upregulated by JIB-04 and the analysis of how these overlap with GC/ookinete specific genes (18, 54), with PbAP2-SP knockout genes (55) and with PfBDP1 target genes (ChIP-Seq) (51); and **4)** GO terms-Up, contains annotation for the 385 genes upregulated by JIB-04 E.

Table S4. Functional groups expressed across IDC and gametocyte/ookinete-specific gene list used in Figures 5 & 6.

Functional groups from literature review used in the transcriptome analysis including fold change (log2) and average expression values (RPKM) of JIB-04 E-treated parasites relative to controls after 6 h. This file includes four tabs: **1)** Functional groups expressed at various times throughout the IDC from (49); **2)** Invasion gene families adapted from Poran and Nötzl et al.; **3)** Genes specifically expressed in gametocytes and ookinetes (18, 54); and **4)** Statistical analysis of the 620 genes deregulated by JIB-04 E compared to each of the three functional group datasets.